Supporting information

Pyrazinyl-functionalized Zr(IV)-MOF for ultrasensitive detection of tyrosine/TNP and efficient CO$_2$/N$_2$ separation

Jin-Min Liu[†][a,b], Jin-Xin Hou[†][a,b], Jie Liu[a,b], Xu Jing[a], Li-Jun Li[a,b] and Jian-Long Du*[a,b]

[a]College of Chemistry & Environmental Science, and Key Laboratory of Chemical Biology of Hebei Province, Hebei University, Baoding 071002, P. R. China

[b]Key laboratory of Medicinal Chemistry and Molecular Diagnosis of Ministry of Education, Hebei University, Baoding 071002, P. R. China

_____

[†]These authors contributed equally to this article.

* Corresponding author. E-mail: dujl@hbu.cn (J.-L. Du).

X-ray data collection

The crystallographic data of **HBU-18** was collected by a Bruker SMART APEX CCD diffractometer using graphite-monochromated Mo-Kα radiation (λ = 0.71073 Å). Data integrating and scaling were conducted by SAINT and SADABS programs. The structure was solved by the direct method (SHELX-2017).[S1] PLANTION SQUEEZE program was used to remove free solvent molecules. The molecular formula was corrected based on element and thermogravimetric analysis. Crystallographic data was displayed in Table S1 and S2. The CCDC reference number for **HBU-18** is 1919374.

Table S1. Crystal data and structure refinements for **HBU-18**.

	HBU-18	After treated by acid (pH= 1)	After treated by base (pH= 11)
Empirical Formula	$C_{32}H_{24}N_2O_{16}Zr_3$		
Formula weight	966.13		
Crystal system	Tetragonal	Tetragonal	Tetragonal
Space group	$I4(1)/amd$		
a (Å)	15.1821(7)	15.14	15.16
b (Å)	15.1821(7)	15.14	15.16
c (Å)	60.416(6)	60.47	60.76
α (°)	90	90	90
β (°)	90	90	90
γ (°)	90	90	90
Volume (Å^3)	13925.7(19)	13861	13962
Z	8		
Dcalc (g cm^{-3})	0.914		
μ (mm^{-1})	0.480		
F(000)	3760		
$R_1{}^a$ / wR$_2{}^b$[I>2sigma(I)]	0.0778/0.2542		
$R_1{}^a$ / wR$_2{}^b$ (all data)	0.1424/0.2898		
GOF on F^2	1.002		

[a]$R_1 = \Sigma(||F_0|-|F_C||)/\Sigma|F_0|$, [b]$wR_2 = [\Sigma w(|F_0|^2-|F_C|^2)^2/\Sigma w(F_0{}^2)]^{1/2}$.

Table S2. Selected bond distances (Å) and bond angles (°) in **HBU-18**.

Zr(1)-O(3)	2.075(4)	Zr(1)-O(1W)	2.221(8)
Zr(1)-O(4)	2.242(4)	Zr(1)-O(1)	2.245(6)
Zr(2)-O(3)	2.044(7)	Zr(2)-O(2)	2.208(5)
Zr(2)-O(4)	2.324(8)		
O(3)[#1]-Zr(1)-O(3)	91.5(4)	O(3)[#1]-Zr(1)-O(1W)	144.8(2)
O(3)-Zr(1)-O(1W)	95.1(3)	O(1W)-Zr(1)-O(1W)[#2]	99.1(5)
O(3)[#1]-Zr(1)-O(4)	69.9(2)	O(3)-Zr(1)-O(4)	72.0(3)
O(1W)-Zr(1)-O(4)	144.7(2)	O(1W)[#2]-Zr(1)-O(4)	78.0(3)
O(4)-Zr(1)-O(4)[#3]	124.1(4)	O(3)-Zr(1)-O(1)[#2]	142.9(2)
O(4)-Zr(1)-O(1)[#2]	134.3(3)	O(3)-Zr(1)-O(1)	79.1(3)
O(1W)-Zr(1)-O(1)	72.2(3)	O(1W)[#2]-Zr(1)-O(1)	74.9(3)
O(4)-Zr(1)-O(1)	73.1(2)	O(1)[#2]-Zr(1)-O(1)	128.3(3)
O(3)-Zr(2)-O(3)[#4]	92.8(4)	O(3)-Zr(2)-O(2)	84.8(2)
O(3)[#4]-Zr(2)-O(2)	143.11(17)	O(2)-Zr(2)-O(2)[#4]	118.2(3)
O(2)-Zr(2)-O(2)[#5]	73.5(3)	O(2)-Zr(2)-O(2)[#6]	75.9(3)
O(2)-Zr(2)-O(4)[#4]	140.43(16)	O(3)-Zr(2)-O(4)	70.79(14)
O(2)-Zr(2)-O(4)	73.7(2)	O(4)[#4]-Zr(2)-O(4)	123.0(4)

Symmetry codes: #1 y+3/4, -x+5/4, -z+3/4; #2 y+3/4, x-3/4, -z+3/4; #3 -y+5/4, x-3/4, -z+3/4; #4 -x+2, -y+1/2, z; #5 -x+2, y, z; #6 x, -y+1/2, z.

Detection limit (LOD) calculation

For calculating detection limit, TNP (10^{-4} M, stock solution) was added to probe (guest-free) (0.20 mg·mL^{-1}) and fluorescent intensities were recorded. By plotting fluorescence intensity (I_0-I) with increasing concentration of nitro-explosives (mM), slope (m) was calculated from the graph. Standard deviation (σ) was calculated from four blank measurements of the probe. Detection limit is calculated based on the formula: ($3\sigma/m$).

Table S3. The calculated limit of detection (LOD) for Tyr and TNP.

Blank readings	Fluorescence intensity			
1-4	1065509.3,	1066326.0,	1066635.7,	1067099.9
5-8	1067288.1,	1067322.3,	1067618.9,	1067764.7
Standard deviation (σ)	751.2			
Slope (m) (FigS6 / S10)	23960.9 (Tyr) / 368303 (TNP)			
Detection limit ($3\sigma/m$)	**94 nM** (Tyr) / **6.2 nM** (TNP)			

Table S4. LUMO and HOMO energies of H$_4$L and different amino acids.

Analytes	H$_4$L	Ser	Tyr	Gly	Trp	Val	Phe
LUMO / eV	-2.87	0.147	-0.017	0.214	-0.35	0.212	-0.085
HOMO / eV	-6.68	-6.49	-5.75	-6.61	-5.49	-6.64	-6.51
Analytes	Pro	Ala	Thr	Met	Leu	Ile	His
LUMO / eV	0.135	0.14	-0.29	-0.097	0.102	0.145	0.16
HOMO / eV	-6.36	-6.46	-6.58	-5.86	-6.68	-6.47	-5.80
Analytes	Lys	Glu	Cys	Asp	Gln	Asn	Arg
LUMO / eV	0.130	-0.134	-0.065	-0.0027	0.020	-0.007	-0.064
HOMO / eV	-6.17	-6.64	-6.88	-6.37	-6.46	-6.42	-5.68

Table S5. A summary of the MOFs for sensing of TNP.

MOF	K_{SV} (M^{-1})	LOD (M)	Medium	Ref.
Zn$_2$(H$_2$L)$_2$(Bpy)$_2$(H$_2$O)$_3$·H$_2$O	1.36×10^4	4.9×10^{-7}	H$_2$O	S2
{[Cd$_{1.5}$(TPO)(bipy)$_{1.5}$]·3H$_2$O}$_{2n}$	2.4×10^5	6.5×10^{-8}	H$_2$O	17
[Tb(1,3,5-BTC)]	3.41×10^4	8.1×10^{-8}	EtOH	S3
Zr$_6$O$_4$(OH)$_4$(L)$_6$ (UiO-67@N)	2.9×10^4	—	H$_2$O	S4
[Zr$_6$O$_4$(OH)$_4$(BTDB)$_6$]·8H$_2$O· 6DMEF	2.49×10^4	1.63×10^{-6}	MeOH	S5
Zr$_6$O$_4$(OH)$_4$(L)$_6$	2.9×10^4	2.6×10^{-6}	H$_2$O	S6
BUT-13	5.1×10^5	4.37×10^{-8}	H$_2$O	S7
HBU-18	$\mathbf{2.46 \times 10^7}$	$\mathbf{6.2 \times 10^{-9}}$	**H$_2$O**	**This work**

Table S6. CO$_2$ uptakes of different MOFs.

MOFs	298 K (cm^3·g^{-1})	Ref.
JUC-MOF57	15	S8
Cu-Sp5	24.8	S9
[Cd$_2$(tdz)$_2$(4,4'-bpy)$_2$]·6.5H$_2$O	29.12	S10
HBU-18	**30.58**	**This work**
[Zr$_6$O$_4$(OH)$_8$(H$_2$O)$_4$(BTEB)$_2$]	42	31
[Zn$_2$(TCA)(BIB)$_{2.5}$]·(NO$_3$)	48.4	S11
Cd-PTC	58	S12
[ZnLi(PTCA)]	60.9	S13

Table S7. Q_{st} values of CO_2 adsorption for some reported MOFs.

MOFs	Q_{st} (kJ/mol)	Ref.
UMCM-1	11.9	S14
MOF-5	16.5	S15
NU 1000	17	S16
SIFSIX-2-Cu	21	S17
IITKGP-5	22.6	S18
IITKGP-6	23	S19
ZTF-1	25.4	S20
Cu-TPBTM	26	S21
SIFSIX-1-Cu	27	S17
PCN-88	27	S22
HBU-18	**27.89**	**This work**
$[Co_2Cl_2(bbta)]$	28	S23
$[Cu(bcppm)H_2O]$	29	S24
$[Cu(Me-4pytrz-ia)]$	30	S25
$\{[Co_2(4,4-bpy)(L)]\cdot H_2O\cdot 0.5(DMF)\}_n$	31.09	S26
ZnPC-2	32	S27
$[Cu_2(L)(H_2O)_2]$	36.4	S28

Table S8. Adsorption capacities of N_2 and CO_2.

	HBU-18	**HBU-18** treated by acid (pH = 1) for 24 h	**HBU-18** treated by base (pH = 11) for 24 h
273 k N_2 uptakes / cm^3/g	6.67	5.02	4.62
273 k CO_2 uptakes / cm^3/g	49.17	65.97	64.60
298 k N_2 uptakes / cm^3/g	2.71	3.82	3.71
298 k CO_2 uptakes / cm^3/g	30.58	38.95	37.69

Table S9. Adsorption selectivity of reported MOFs for CO_2/N_2 (15:85) at 298 K.

MOFs	CO_2/N_2	Ref.
SIFSIX-2-Cu	13.7	S29
Cu-BTTri	21	S30
JUC-141	27.6	S31
TIFSIX-1-Cu	30	S32
HBU-18	**41.79**	**This work**
ZIF-78	50.1 / 296K	S33
Cu-TDPAT	57.8 / 296K	S34
USTA-85a	62.5 / 296K	S35
Bio-MOF-11	79.5 / 296K	S34

(a) (b)
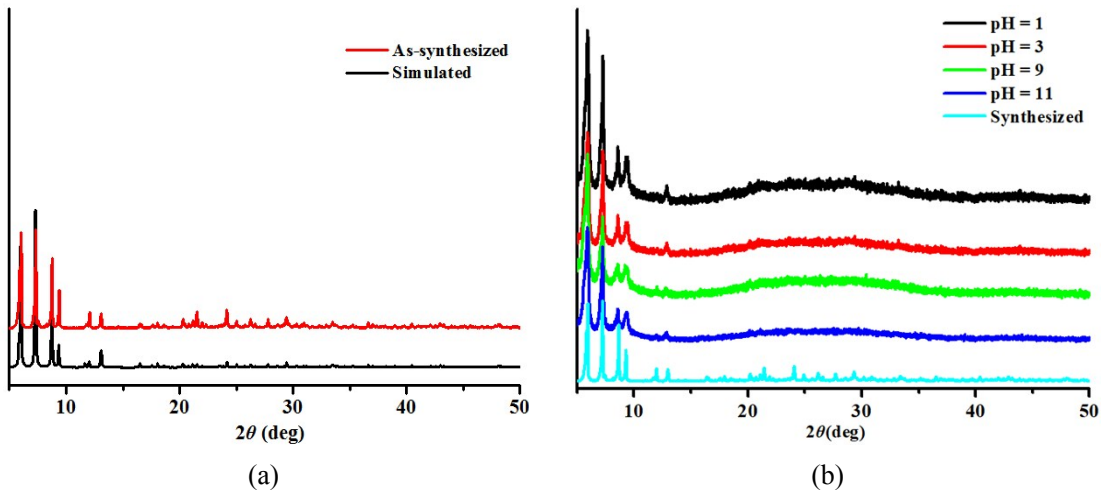
Fig. S1 (a) PXRD patterns of **HBU-18**; (b) PXRD patterns of **HBU-18** after immersed in aqueous solution for 24 h.
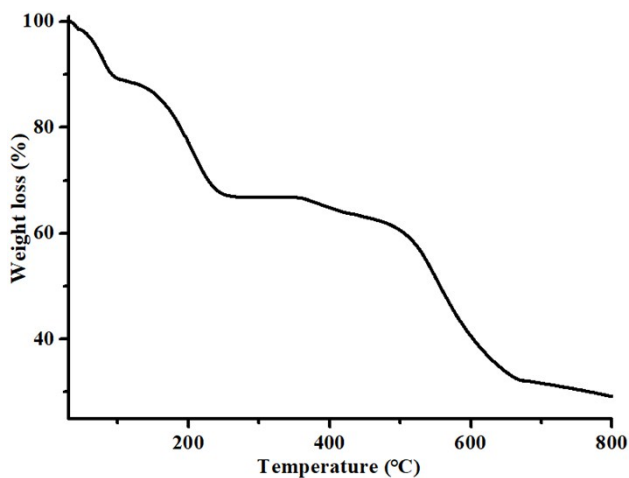
Fig. S2 TG curve of **HBU-18**
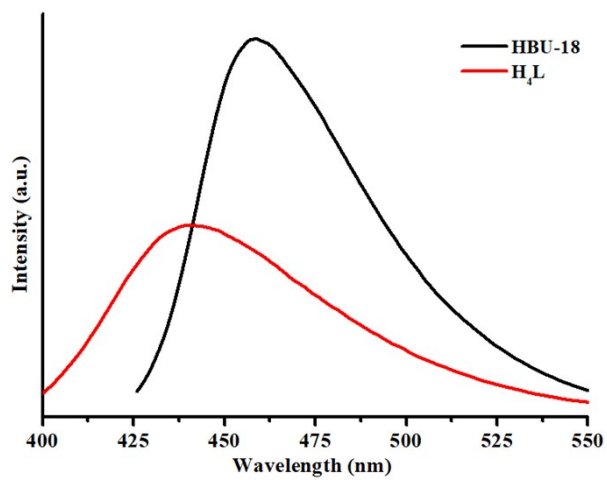
Fig. S3 Fluorescence spectra of H$_4$**L** and **HBU-18** in the solid state.
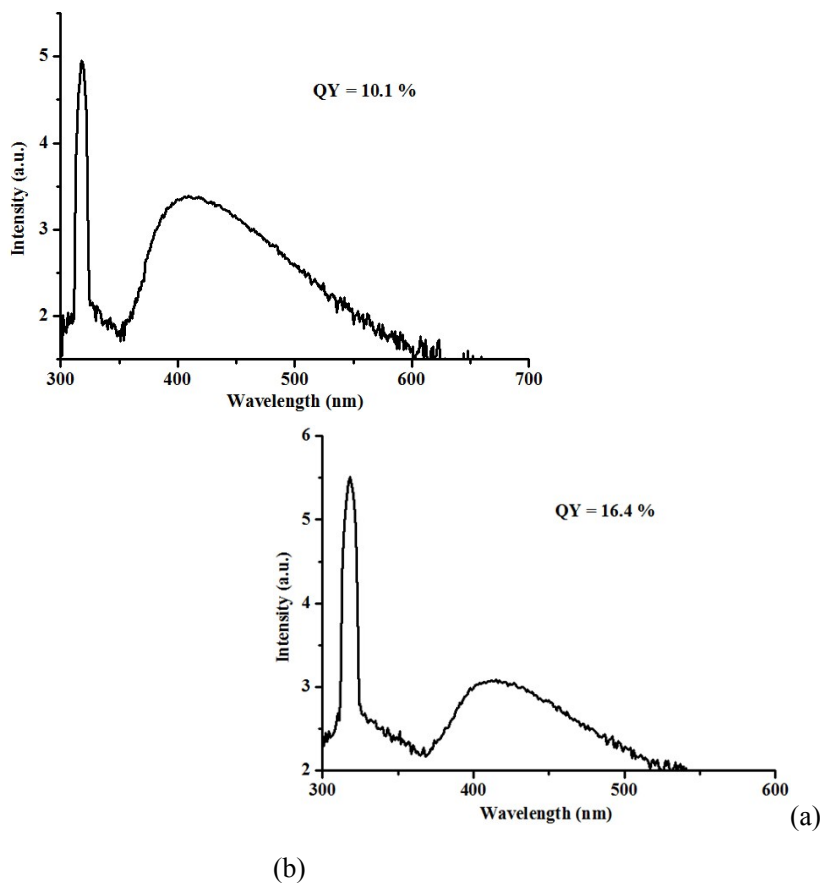
Fig. S4 Fluorescence quantum yield of H$_4$**L** (a) and **HBU-18** (b) in aqueous solution.
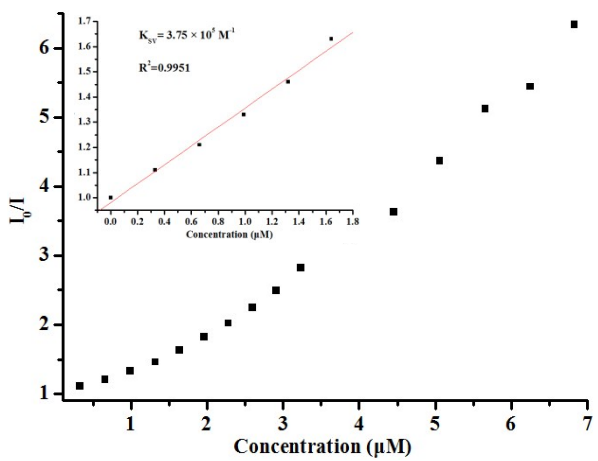
**Fig. S5** Stern-Volmer (SV) plot of Tyr.
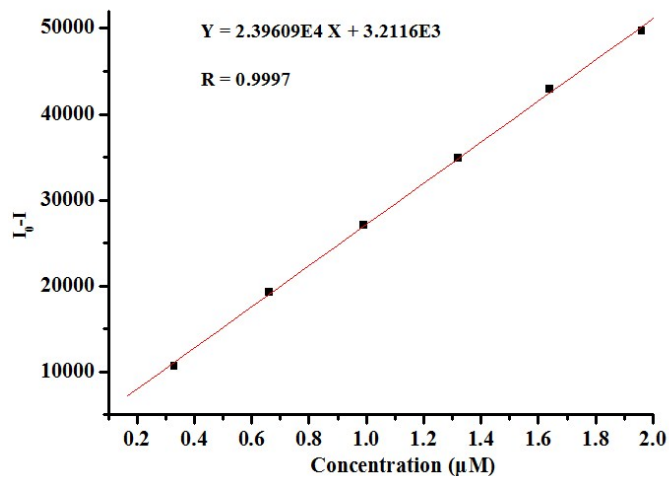
Fig. S6 Linear fitting between I_0-I and the concentration of Tyr.
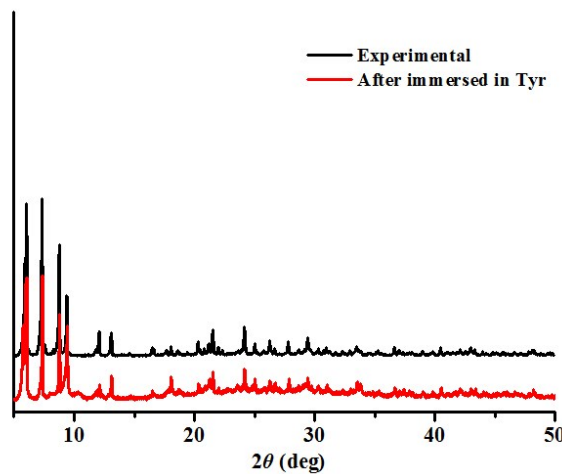
Fig. S7 PXRD patterns of **HBU-18** before and after immersed in the solution of Tyr (10^{-4} M).
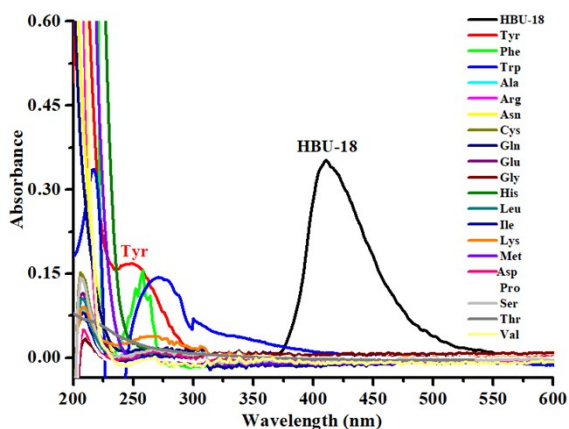
Fig. S8 UV-vis spectra of amino acids and emission spectrum of **HBU-18**.
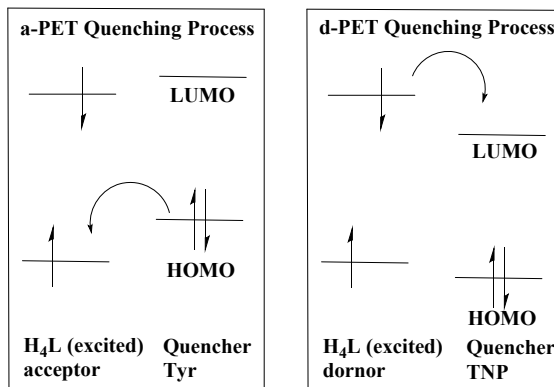
Fig. S9 a-PET and d-PET quenching process.
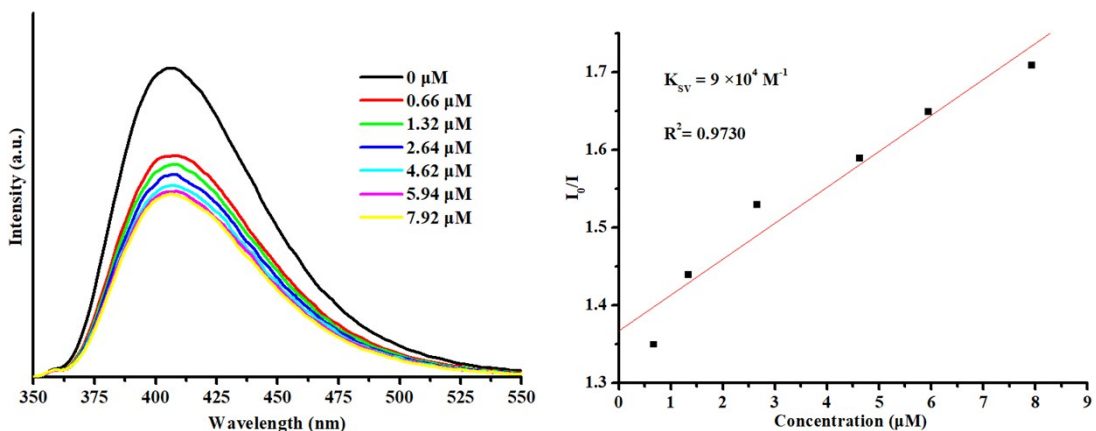
Fig. S10 Fluorescence detection of Tyr after **HBU-18** immersed in acidic solution (pH = 1).
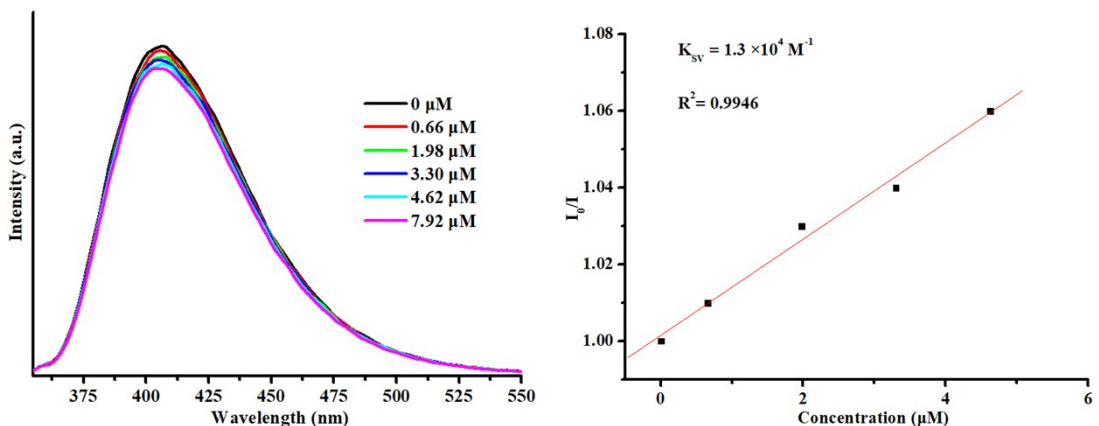
Fig. S11. Fluorescence detection of Tyr after **HBU-18** immersed in basic solution (pH = 11).
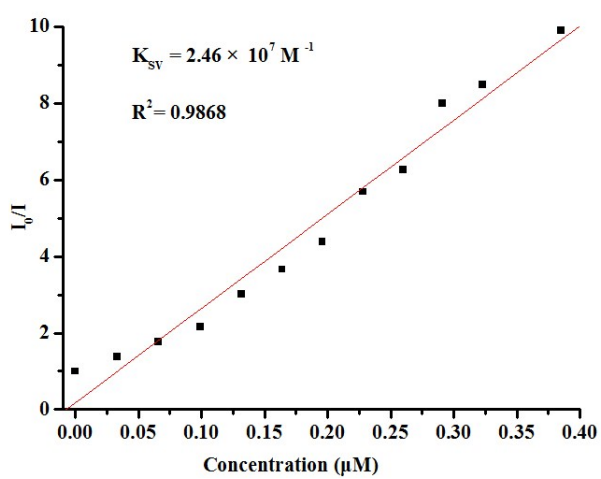
Fig. S12 Stern-Volmer (SV) curve after sensing of TNP.
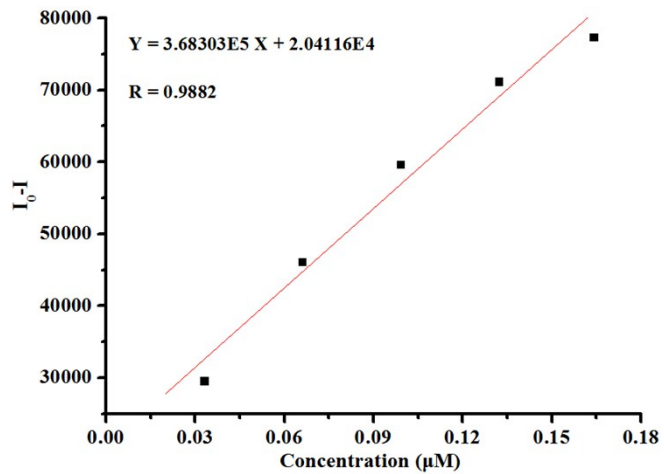
**Fig. S13** Linear fitting between I_0-I and the concentration of TNP.
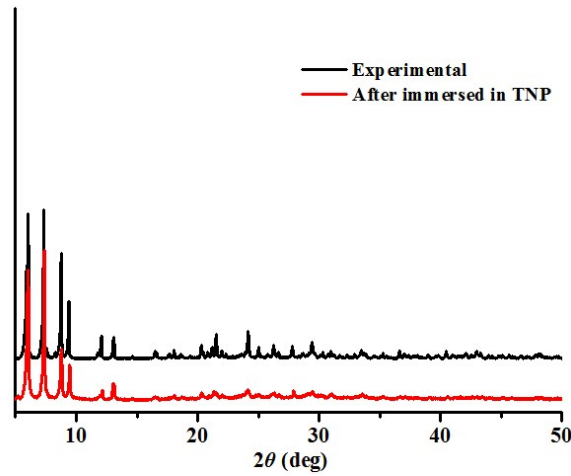
**Fig. S14**. PXRD patterns of **HBU-18** before and after immersed in the solution of TNP (10^{-5} M).
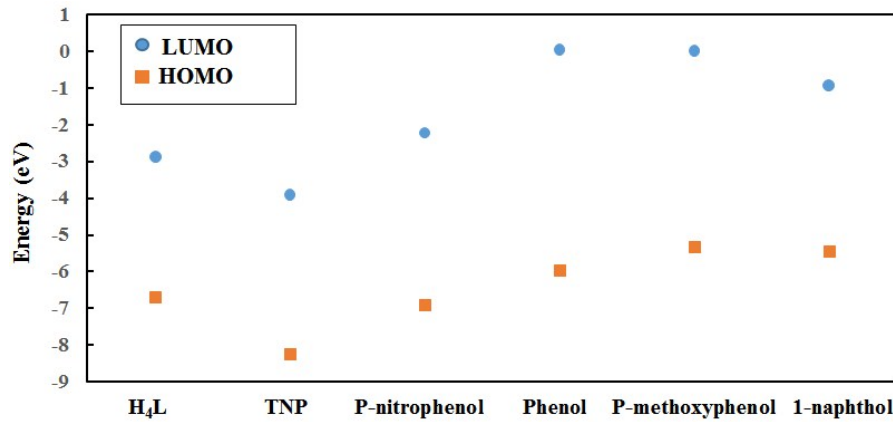
**Fig. S15**. LUMO and HOMO energy levels of H_4L ligand and analytes.
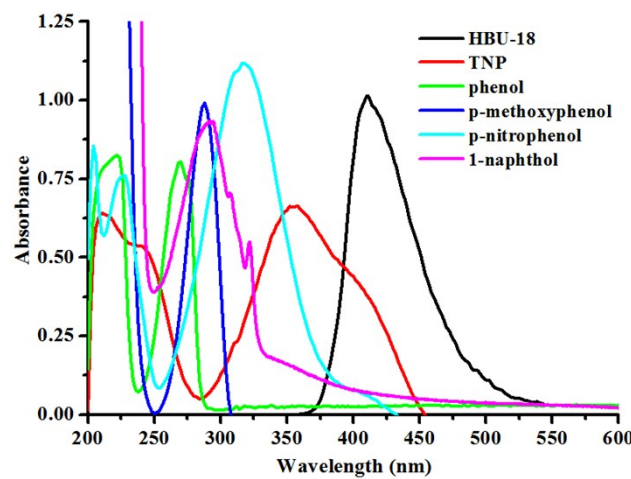
Fig. S16. UV-vis spectra of analytes and fluorescence spectrum of **HBU-18**.
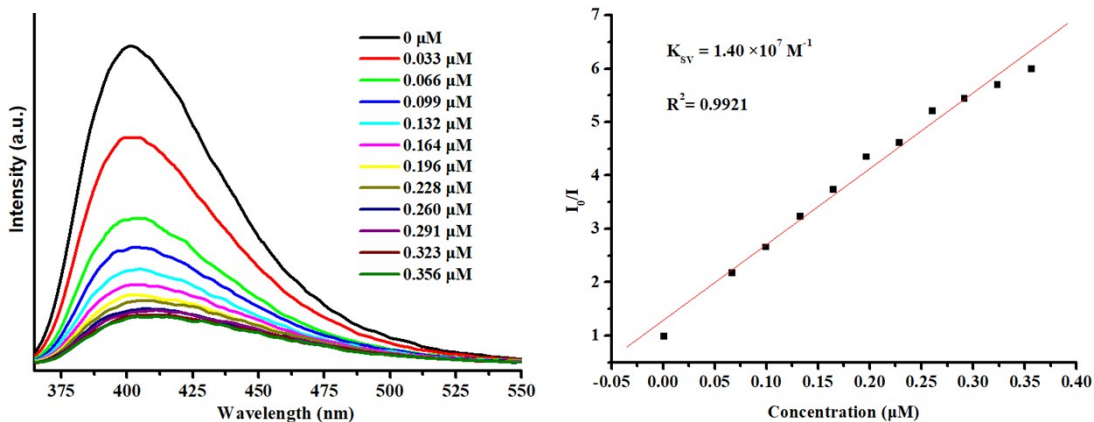
Fig. S17. Fluorescence detection of TNP after **HBU-18** immersed in acidic solution (pH = 1).
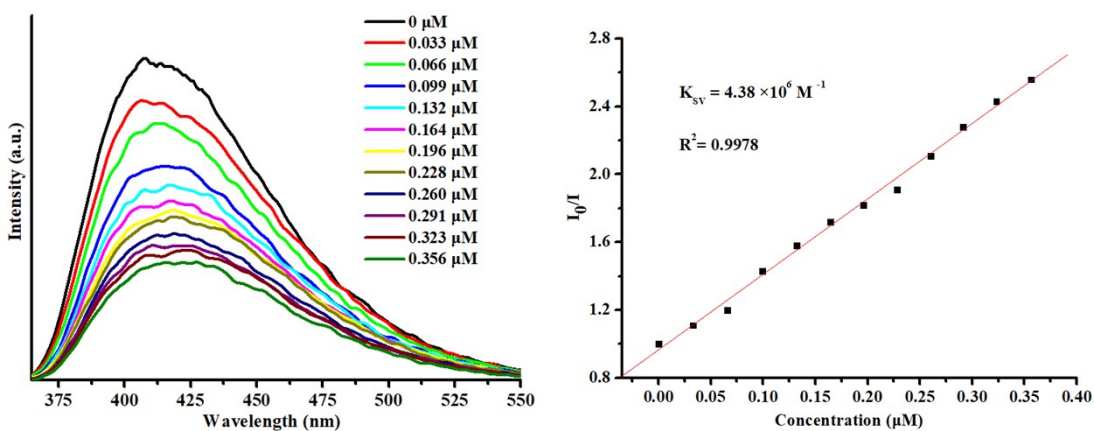

**Fig. S18**. Fluorescence detection of TNP after **HBU-18** immersed in basic solution (pH = 11).
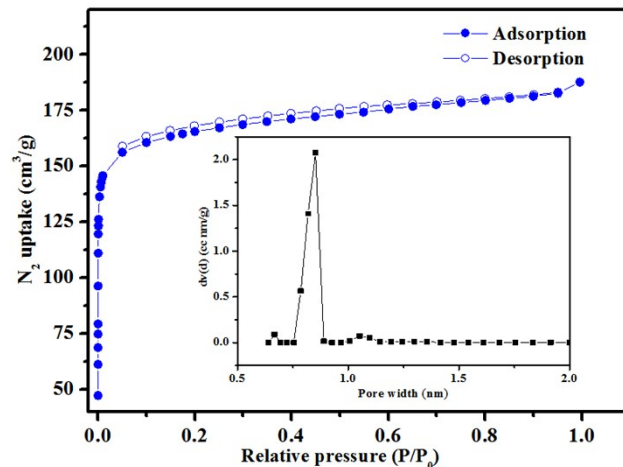
Fig. S19. N_2 adsorption-desorption isotherms of **HBU-18**.

Calculation of sorption heat for CO_2 uptake using Virial 2 model

$$lnP = lnN + 1/T \sum_{i=0}^{m} aiN^i + \sum_{i=0}^{n} biN^i$$

$$Q_{st} = -R \sum_{i=0}^{m} aiN^i$$

The above equation was applied to fit the combined CO_2 isotherm data for desolvated **HBU-18** at 273 and 298 K, where P is the pressure, N is the adsorbed amount, T is the temperature, ai and bi are virial coefficients, and m and n are the number of coefficients used to describe the isotherms. Q_{st} is the coverage-dependent enthalpy of adsorption and R is the universal gas constant.
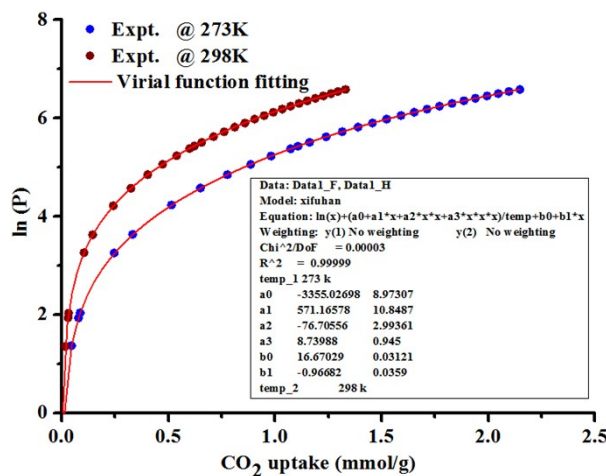

**Fig. S20**. CO_2 adsorption isotherms of **HBU-18** at 273 and 293 K fitted using the virial equation.
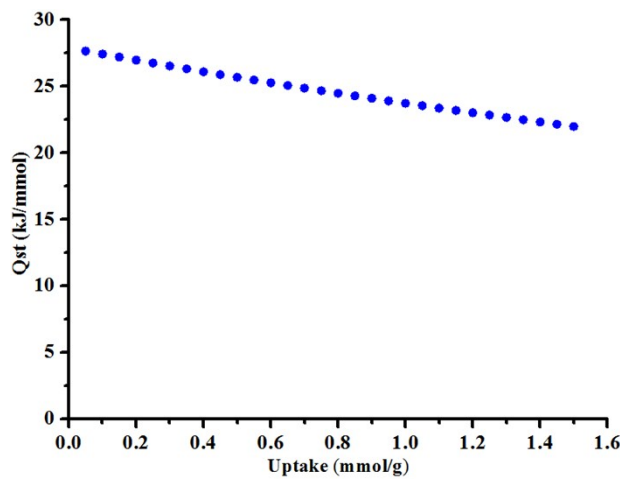
**Fig. S21**. Isosteric heat of CO_2 (Q_{st}) for **HBU-18**.
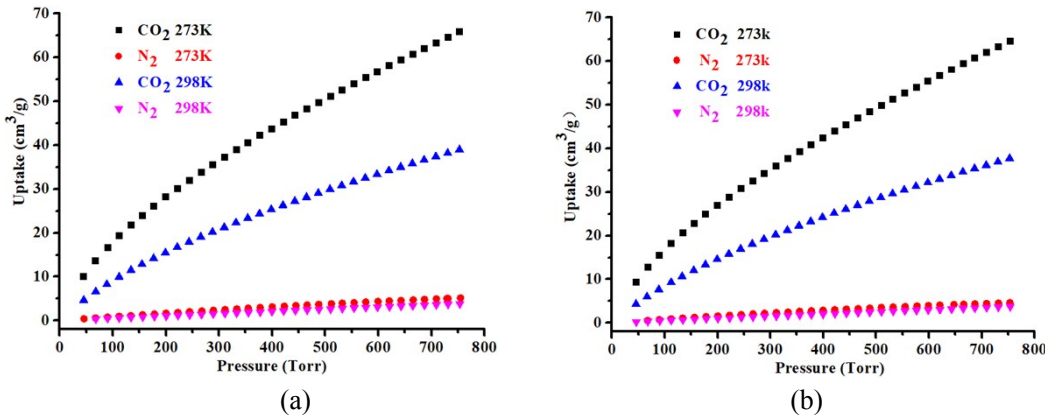
Fig. S22. CO_2 and N_2 adsorption isotherms at 298 K and 273 K: (a) activated by acid (pH = 1); (b) activated by base (pH = 11).

Calculation of CO_2/N_2 Selectivity (IAST Selectivity):

Adsorption isotherms and gas selectivities of mixed CO_2/N_2 (5:95, 15:85, 25:75, 50:50) at different temperatures were calculated based on the ideal adsorbed solution theory (IAST) proposed. In order to calculate the selective sorption performance of **HBU-18** toward the separation of binary mixed gases, the parameters fitted from the single component CO_2 and N_2 adsorption isotherms based on the single-site Langmuir−Freundlich (SSLF) model and were used in the IAST calculations as given below in detail.

$$y = \frac{q * b * x^{1/t}}{1 + q * b * x^{1/t}}$$

Where x is the pressure of the bulk gas at equilibrium with the adsorbed phase (kPa); y is the adsorbed amount per mass of adsorbent (mmol/g), q is the saturation capacities of site 1 (mmol/g); b is the affinity coefficients of site 1 (1/kPa), t represent the deviations from an ideal homogeneous surface.

The predicted adsorption selectivity is defined as

$$S = (x1/y1)/(x2/y2)$$

here xi and yi are the mole fractions of component i (i = 1, 2) in the adsorbed and bulk phases, respectively. The IAST calculations were carried out for a binary mixture containing 15% CO_2 (y1) and 85% N_2 (y2), which is typical of flue gases.


14
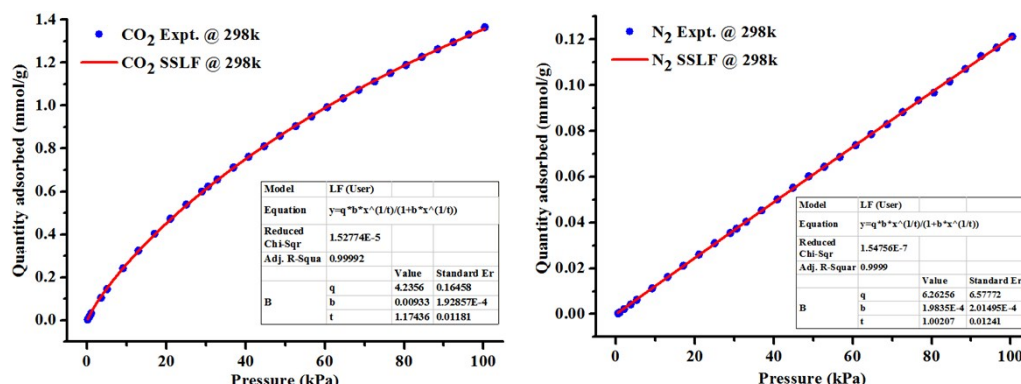
Fig S23. Single-site Langmuir-Freundlich fitting (red line) for CO_2 and N_2 (blue circle) isotherms.
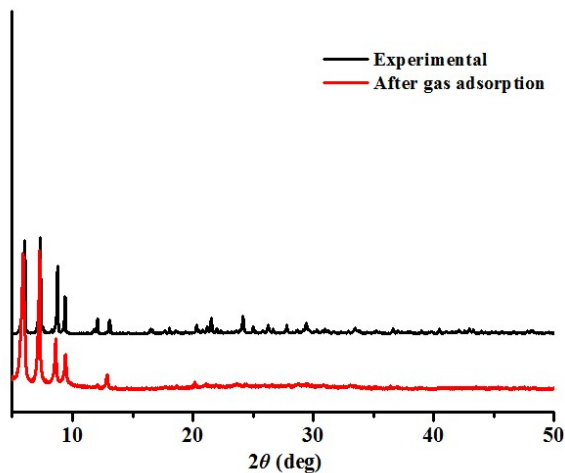

Fig. S24. PXRD patterns of **HBU-18** before and after gas adsorption.

References

S1. G. M. Sheldrick, *Acta Cryst. C.*, 2015, **71**, 3-8.

S2. Y. Deng, N. Chen, Q. Li, X. Wu, X. Huang, Z. Lin and Y. Zhao, *Cryst. Growth Des.*, 2017, **17**, 3170-3177.

S3. J. D. Xiao, L. G. Qiu, F. Ke, Y. P. Yuan, G. S. Xu, Y. M. Wang and X. Jiang, *J. Mater. Chem. A*, 2013, **1**, 8745-8752.

S4. S. S. Nagarkar, B. Joarder, A. K. Chaudhari, S. Mukherjee and S. K. Ghosh, *Angew. Chem. Int. Ed.*, 2013, **52**, 2881-2885.

S5. M. SK and S. Biswas, *CrystEngComm*, 2016, **18**, 3104-3113.

S6. S. S. Nagarkar, A. V. Desai and S. K. Ghosh, *Chem. Commun.*, 2014, **50**, 8915-8918.

S7. B. Wang, X. L. Lv, D. W. Feng, L. H. Xie, J. Zhang, M. Li, Y. B. Xie, J. R. Li and H. C. Zhou, *J. Am. Chem. Soc.*, 2016, **138**, 6204-6216.

S8. S. Liu, S. Yao, B. Liu, X. D. Sun, Y. Yuan, G. H. Li, L. R. Zhang and Y. L. Liu, *Dalton Trans.*, 2019, **48**, 1680-1685.

S9. I. Kochetygov, S. Bulut, M. Asgari and W. L. Queen, *Dalton Trans.*, 2018, **47**, 10527-10535.

S10. A. Gogia and S. K. Mandal, *Dalton Trans.*, 2019, **48**, 2388-2398.

S11. C. Yao, S. Zhou, X. Kang, Y. Zhao, R. Yan, Y. Zhang and L. Wen, *Inorg. Chem.*, 2018, **57**, 11157-11164.

S12. L. Hu, X.-J. Hong, X.-M. Lin, J. Lin, Q.-X. Cheng, B. Lokesh and Y.-P. Cai, *Cryst. Growth*

Des., 2018, **18**, 7088-7093.

S13. Y. L. Huang, D. C. Zhong, L. Jiang, Y. N. Gong and T. B. Lu, *Inorg. Chem.*, 2017, **56**, 705-708.

S14. B. Mu, P. M. Schoenecker and K. S. Walton, *J. Phys. Chem. C*, 2010, **114**, 6464-6471.

S15. J. S. Choi, W. J. Son, J. Kim and W. S. Ahn, *Micropor. Mesopor. Mat.*, 2008, **116**, 727-731.

S16. P. Deria, J. E. Mondloch, E. Tylianakis, P. Ghosh, W. Bury, R. Q. Snurr, J. T. Hupp and O. K. Farha, *J. Am. Chem. Soc.*, 2013, **135**, 16801-16804.

S17. S. D. Burd, S. Ma, J. A. Perman, B. J. Sikora, R. Q. Snurr, P. K. Thallapally, J. Tian, L. Wojtas and M. J. Zaworotko, *J. Am. Chem. Soc.*, 2012, **134**, 3663-3666.

S18. A. Pal, S. Chand, S. M. Elahi and M. C. Das, *Dalton Trans.*, 2017, **46**, 15280-15286.

S19. A. Pal, S. Chand and M. C. Das, *Inorg. Chem.*, 2017, **56**, 13991-13997.

S20. T. Panda, P. Pachfule, Y. Chen, J. Jiang and R. Banerjee, *Chem. Commun.*, 2011, **47**, 2011-2013.

S21. B. Zheng, J. Bai, J. Duan, L. Wojtas and M. J. Zaworotko, *J. Am. Chem. Soc.*, 2011, **133**, 748-751.

S22. J.-R. Li, J. Yu, W. Lu, L.-B. Sun, J. Sculley, P. B. Balbuena and H.-C. Zhou, *Nat. Commun.*, 2012, **4**, 1538.

S23. P.-Q. Liao, H. Chen, D. D. Zhou, S.-Y. Liu, C. T. He, Z. Rui, H. Ji, J.-P. Zhang and X.-M. Chen, *Energy Environ. Sci.*, 2015, **8**, 1011-1016.

S24. W. M. Bloch, R. Babarao, M. R. Hill, C. J. Doonan and C. J. Sumby, *J. Am. Chem. Soc.*, 2013, **135**, 10441-10448.

S25. D. Lässig, J. Lincke, J. Moellmer, C. Reichenbach, A. Moeller, R. Gläser, G. Kalies, K. A. Cychosz, M. Thommes, R. Staudt and H. Krautscheid, *Angew. Chem. Int. Ed.*, 2011, **50**, 10344-10348.

S26. V. Gupta and S. K. Mandal, *Dalton Trans.*, 2019, **48**, 415-418.

S27. Y. Ling, M. Deng, Z. Chen, B. Xia, X. Liu, Y. Yang, Y. Zhou and L. Weng, *Chem. Commun.*, 2013, **49**, 78-80.

S28. C.-Y. Gao, H.-R. Tian, J. Ai, L.-J. Li, S. Dang, Y.-Q. Lan and Z.-M. Sun, *Chem. Commun.*, 2016, **52**, 11147-11150.

S29. P. Nugent, Y. Belmabkhout, S. D. Burd, A. J. Cairns, R. Luebke, K. Forrest, T. Pham, S. Ma, B. Space, L. Wojtas, M. Eddaoudi and M. J. Zaworotko, *Nature*, 2013, **495**, 80-84.

S30. A. Demessence, D. M. D'Alessandro, M. L. Foo and J. R. Long, *J. Am. Chem. Soc.*, 2009, **131**, 8784-8786.

S31. N. Zhao, F. Sun, P. Li, X. Mu and G. Zhu, *Inorg. Chem.*, 2017, **56**, 6938-6942.

S32. P. Nugent, V. Rhodus, T. Pham, B. Tudor, K. Forrest, L. Wojtas, B. Space and M. Zaworotko, *Chem. Commun.*, 2013, **49**, 1606-1608.

S33. A. Phan, C. J. Doonan, F. J. Uribe-Romo, C. B. Knobler, M. O'Keeffe and O. M. Yaghi, *Acc Chem Res*, 2010, **43**, 58-67.

S34. S. Xiang, Y. He, Z. Zhang, H. Wu, W. Zhou, R. Krishna and B. Chen, *Nat. Commun.*, 2012, **3**, 954.

S35. O. Alduhaish, H. Wang, B. Li, H. D. Arman, V. Nesterov, K. Alfooty and B. Chen, *Chempluschem*, 2016, **81**, 764-769.